NONLINEAR FINITE ELEMENT ANALYSES OF REINFORCED CONCRETE SLABS: COMPARISON OF SAFETY FORMATS

B.BELLETTI[*], C.DAMONI[†], M.A.N. HENDRIKS[+] AND J.A. DEN UIJL[#]

[*] University of Parma
Parco Area delle Scienze 181/A,43100 Parma, Italy
e-mail: beatrice.belletti@unipr.it

[†] University of Parma
Parco Area delle Scienze 181/A,43100 Parma, Italy
e-mail: cecilia.damoni@nemo.unipr.it

[+] Delft University of Technology
Stevinweg 1, 2628CN Delft, The Netherlands
e-mail: M.A.N.Hendriks@tudelft.nl

[#] Delft University of Technology
Stevinweg 1, 2628CN Delft, The Netherlands
e-mail: j.a.denuijl@tudelft.nl

Key words: reinforced concrete slabs, nonlinear finite element analyses, shear resistance evaluation, guidelines, safety levels

Abstract: According to the new fib Model Code 2010 the design shear resistance of a reinforced concrete (RC) structure can be evaluated through analytical and numerical calculation methods that fall into four different levels of approximations; the complexity and the accuracy of the calculated shear resistance increases with increasing the level of approximation. Nonlinear finite element (NLFE) analyses belong to the highest level of approximation (Level IV) thanks to their advantage to take into account real material properties and "hidden" capacities of the structure. Nevertheless, even if NLFE analyses are more and more becoming an usual instrument in the daily design process, building codes do not provide specific guidance on how to perform these analyses and if appropriate checks are not done on the model used, a big scatter in the results obtained can be detected. For this reason the Dutch Ministry of Transport, Public Works and Water Management is running a project to re-evaluate the carrying capacity of existing bridges and viaducts (e.g. reinforced and prestressed concrete beams and slabs) through NLFE analyses and published in a document containing guidelines for nonlinear finite element analyses to be followed by users in order to reduce model and users factors. In the paper several reinforced concrete slabs have been analyzed through analytical and numerical procedures according to the Model Code 2010 prescriptions and following the Dutch guidelines. The analytical and numerical results obtained have been compared with experimental results.

Parametric studies have also been carried out on the slabs in order to focus on the main sensitive parameters that influence the results obtained from numerical simulations and in order to obtain reliable and, at the same time, safe results. The main indications of the guidelines for reinforced concrete slabs are presented in the paper.

1 INTRODUCTION

The Dutch Ministry of Transport, Public Works and Water Management is running a project to re-evaluate the load carrying capacity of existing bridges and viaducts in the whole country because of the increase of traffic and the reallocation of emercency lanes to traffic lanes. For a certain amount of Dutch bridges and other infrastructures the safety verifications are not satisfied if the usual analytical procedures, proposed by the current norms (e.g. [1]), are adopted for the calculations. For this reason The Dutch Ministry of Transport, Public Works and Water Management proposed to make a structural assessment of existing structures through the use of nonlinear finite element analyses with the final release of a document containing guidelines for nonlinear finite element (NLFE) analyses of reinforced and prestressed concrete elements [2]. Previous studies of the authors specifically deal with indications of the guidelines for reinforced and prestressed beams [3], [4]. In the present paper the focus is on slabs.

The guidelines not only contain indications on the modeling of structures through NLFE analyses but also on the way to present the results in order to facilitate the preparation of technical reports and the reviewing by other professionals. The focus is on the analysts skills in order to control the results from NLFE analyses without "a priori" accepting these results

NLFE analyses, which are more and more becoming a usual instrument in the daily design process, can in fact take into account hidden capacities of the structures and offer refined modelling based on realistic material properties. Nevertheless the power of NLFE analyses does not have to be overestimated. The results of NLFE analyses strongly depend on the modelling choices and therefore a big scatter in the results for the same structure analyzed by several analysts can be detected.

For this reason the development of guidelines for NLFE analyses to be followed by all users in order to obtain reliable and, at the same time, safe results is of big importance. The project well matches with the philosophy of the new Model Code 2010 [5] for the structural assessment of existing structures.

According to this code the design shear resistance of RC structures can be evaluated through analytical and numerical calculation methods that fall into four levels of approximations: by increasing the level of approximation the complexity and the accuracy of the results obtained increases. Level of approximation I, II and III refer to analytical calculation methods while the highest level, level IV, refers to NLFE analyses. The results obtained from NLFE analyses are reduced in order to obtain the same safety level as for the analytical calculations. To this aim, within level IV, the new Model Code 2010 proposes three alternative safety formats methods to elaborate the results of NLFE analyses: the Partial Factor method (PF), the Global Resistance Factor method (GRF) and the Estimation of Coefficient of Variation of resistance method (ECOV).With this the MC2010 is in advance with respect of most other codes.

In the current paper the shear resistance of three concrete slabs has been evaluated through the analytical and numerical procedures based on the levels of approximation proposed by the new Model Code 2010 and the results obtained have been compared with the experimental results performed at Stevin Laboratory [6].

Shear resistance has been achieved by nonlinear finite element analyses carried out with the finite element code DIANA [7]. However the guidelines [2] are valid any commercial finite element code.

Parametric studies have been carried out on the slabs in order to validate the numerical model and for the application of the safety formats methods. The parametric studies investigate the effects that the most sensitive parameters of the constitutive model, like the aggregate interlock effect, the reduction of the compressive strength due to lateral cracking,

1

the Poisson effect and, the influence of the fracture energy , have on the results.

2   CASE STUDIES

  In the paper three reinforced concrete slabs denoted as S1T1, S1T2 and S4T1, experimentally tested at the Stevin laboratory [6] are analyzed. In Figure 1 an overview of the slabs is presented with indication of the reinforcement layout, the support details and the loading scheme. Each slab is constrained by a simple support, a continuous support and three prestressed dywidag bars (denoted as Support 3 in Figure 1). Between the supports and the concrete slab layers of felt and plywood were inserted. In Figure 2 the experimental set-up of S1T1 slab is shown. The mean mechanical properties of concrete measured during the experimental test, the indication of the type of failure detected and the experimental ultimate load value ($P_{u,exp}$) are summarized in Table 1. In Table 2 the mean mechanical properties of steel are reported.
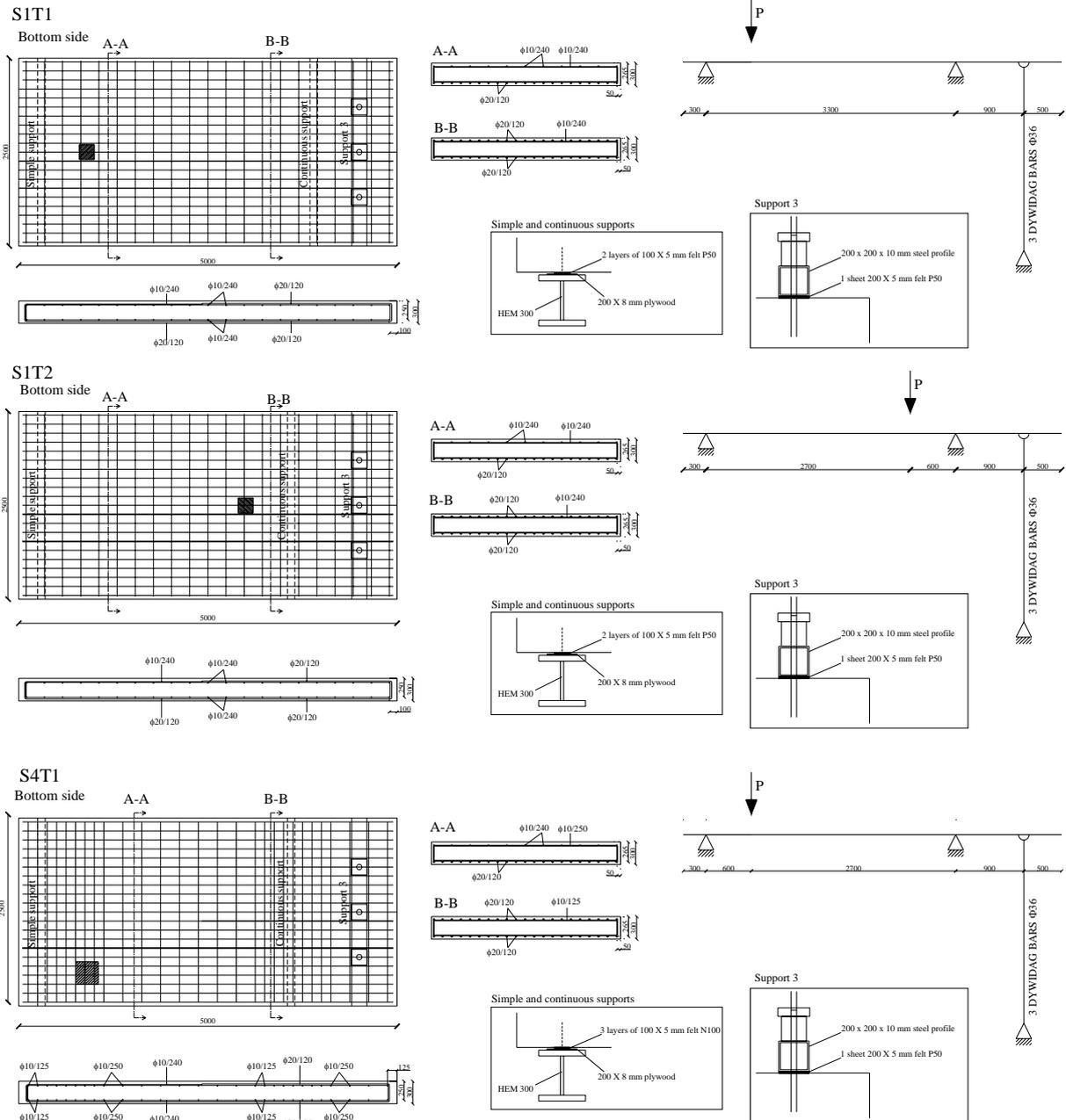
Figure 1: Case studies: S1T1, S1T2, S4T1.

One way shear failure mode was experimentally observed for all three slabs. In Figure 3, Figure 4 and Figure 5 the experimental crack pattern is shown for the S1T1, S1T2 and S4T1 slab, respectively. In Figure 6 the experimental stress-strain relationships of the felt-plywood stacks and felt placed at the support-slab interface are plotted.

Table 1: Mean mechanical properties of concrete, failure mode and experimental ultimate load.

	E_c (Mpa)	f_c (Mpa)	f_t (Mpa)	Failure	$P_{u,exp}$ (KN)
S1T1	30910	29.7	2.8	OWS[*]	954
S1T2	30910	29.7	2.8	OWS[*]	1023
S4T1	34930	42.9	3.8	OWS[*]	1160

[*]OWS=One Way Shear

Table 2: Mean mechanical properties of steel.

	E_s (Mpa)	f_y (Mpa)	F_{pe}[*] (KN)
$\phi 10$	210000	537	-
$\phi 20$	210000	541	-
$3\phi 36$	210000	1000	3·15

F_{pe}[*] = prestressing force

Figure 2: Experimental set-up of S1T1 slab.
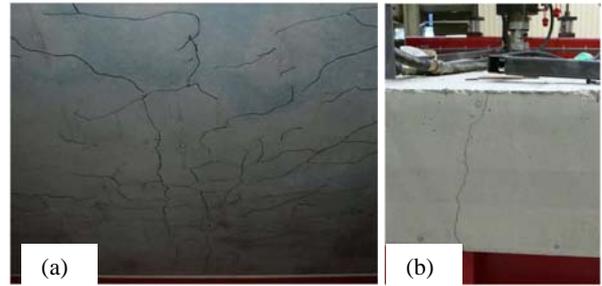
Figure 3: Experimental crack pattern of S1T1 slab (a) at bottom side, (b) on the front face.
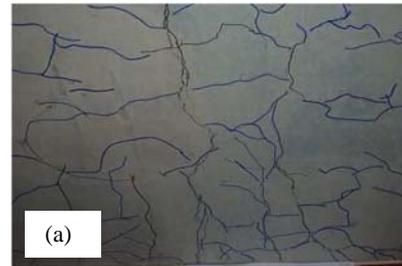
Figure 4: Experimental crack pattern of S1T2 slab (a) at bottom side, (b) on the front face.

Figure 5: Experimental crack pattern of S4T1 slab on the front face.
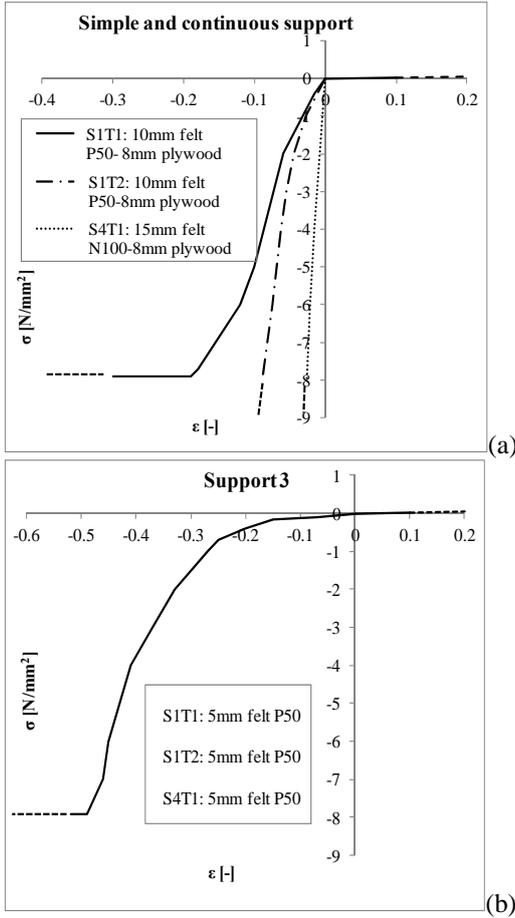
Figure 6: Stress-strain relationship determined experimentally of (a) felt/plywood and (b) felt.

3 DESIGN SHEAR RESISTANCE EVALUATION WITH LEVELS OF APPROXIMATIONS

As mentioned in section 1 the new Model Code 2010 [5] proposes different calculation methods for the evaluation of the design shear resistance of reinforced concrete structures, falling into four different levels of approximations. Level I, II and III refer to analytical procedures while Level IV refers to numerical procedures, which results are obtained through NLFE analyses. The results obtained from NLFE analyses are reduced through safety coefficients in order to obtain the design shear resistance having the same safety level of Level I, II, III.

3.1 Analytical procedure

The design shear resistance of reinforced slabs without shear reinforcement is

calculated as the design shear resistance of beams without shear reinforcement for which only level I and II are provided. In the paper beside the design shear resistance calculated with the levels of approximation, the design punching resistance is calculated following both Eurocode 2 prescriptions [1] and Regan's formulations [8] for loads near supports. In Table 3 the design load values corresponding to the design shear resistances and to the punching resistance are summarized. In Table 3 it is shown that, for all slabs, the design punching resistance is higher than the shear resistance so that, even according to analytical procedures, the failure is due to one-way shear rather than punching failure. The analytical failure mode is in accordance with the experimental failure and the failure detected from nonlinear finite element analyses, as shown in the following sections.

Table 3: Deasign load values in [kN] corresponding to the design shear and design punching resistances.

	Shear MC 2010		Punching	
	Level I	Level II	Regan	EC2
S1T1	204.8	400.6	472.1	542.0
SIT2	161.6	489.4	472.1	542.0
S4T1	229.8	421.2	512.6	498.3

3.1.1 Design shear resistance

As a general rule, Level of approximation I may be used for the conception or the design of a new structure and Level II is appropriate for the design of a new structure as well as for a general or brief assessment of existing structures.

The design shear resistance of a slab without shear reinforcement is calculated as:

$$V_{Rd,c} = k_v \frac{\sqrt{f_{ck}}}{\gamma_c} z b_{eff} \qquad (1)$$

where:

$$\begin{cases} k_{v,\,Level\,I} = \dfrac{180}{1000 + 1.25z} \\ k_{v,\,Level\,II} = \dfrac{0.4}{1 + 1500\varepsilon_x} \cdot \dfrac{1300}{1000 + k_{dg}z} \end{cases} \qquad (2)$$

$$\varepsilon_x = \frac{1}{2E_s A_s} \left(\frac{M_{Ed}}{z_1} + V_{Ed} \right) \qquad (3)$$

$$k_{dg} = \frac{32}{16 + d_g} \geq 0.75 \qquad (4)$$

ε_x is the strain at mid-depth evaluated through an iterative procedure, z is the shear depth taken equal to *0.9d* and b_{eff} is the effective slab width.

It is well known that for a correct design of a slab it is essential to consider the stress redistribution and just a strip of the slab width participates to the shear resistance mechanism. Several works available in literature give different interpretations on how to determine the effective width and several experimental tests have been carried out on slabs [8]. In the current paper the effective width schematized in Figure 7 has been considered in the calculation. The assumption made is in agreement with experimental observations.
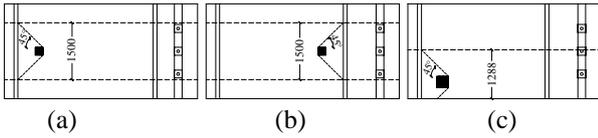
Figure 7: Effective width determination for (a) S1T1 slab, (b) S1T2 slab, (c) S4T1 slab.

3.1.2 Design punching resistance

In eq. (5)-(8) the design punching resistance calculated according to Eurocode 2 prescriptions is given:

$$V_{Rdc} = v_{Rdc} \cdot u \cdot d_{eff} \qquad (5)$$

where

$$v_{Rdc} = C_{Rd,c} k (100 \cdot \rho \cdot f_{ck})^{1/3} \qquad (6)$$

$$C_{Rd,c} = 0.18 / \gamma_c = 0.18 / 1.5 = 0.12 \qquad (7)$$

$$k = 1 + \sqrt{\frac{200}{d_{eff}}} \qquad (8)$$

In eq. (9) the design punching resistance calculated according to Regan's formulation is reported:

$$P_R = P_{R1} + P_{R2} \qquad (9)$$

Eq. (10) provides the resistance value P_{R2} which is referred to the perimeter side parallel and next to the support (u_2). Eq. (11) provides

the resistance value P_{R1} referred to the remaining part of the perimeter (u_1).

$$P_{R2} = \frac{2d_l}{a_v} \cdot \xi_{sl} \cdot v_{cl} \cdot u_2 \cdot d_l \qquad (10)$$

$$P_{R1} = \xi_{sl} \cdot v_{cl} \cdot u_2 \cdot d_l + 2 \cdot \xi_{st} \cdot v_{ct} \cdot u_1 \cdot d_t \qquad (11)$$

where d_l and d_t are the effective depth of the longitudinal and transversal bars and a_v is the distance from the support to the point load application. The variables of eq. (10) and (11) are listed in eq. (12)-(15).

$$\xi_{sl} = \sqrt[4]{\frac{500}{d_l}} \qquad (12)$$

$$\xi_{st} = \sqrt[4]{\frac{500}{d_t}} \qquad (13)$$

$$v_{cl} = \frac{0.27}{\gamma_m} \sqrt[3]{100 \rho_l f_{ck}} \qquad (14)$$

$$v_{ct} = \frac{0.27}{\gamma_m} \sqrt[3]{100 \rho_t f_{ck}} \qquad (15)$$

3.2 Numerical procedures

As already mentioned in the introduction, within Level IV, the new fib Model Code 2010 [5] proposes three different safety formats methods for the evaluation of the design shear resistance through NLFE analyses: the Partial Factor method (PF), the Global Resistance Factor method (GRF) and the Estimation of Coefficient of Variation of resistance method (ECOV).

The PF method provides that design mechanical properties of materials, evaluated according to the fib Model Code prescriptions from the characteristic mechanical properties, are used as input data, so that the shear resistance obtained from the analysis (R_d) is already the design shear resistance:

$$R_d = R(f_d, ...) \qquad (16)$$

The GRF method provides that mean mechanical properties of materials, evaluated from the characteristic mechanical properties according to the fib Model Code prescriptions, are used as input data. The global resistance of the structure R_d is considered a random variable so that the effects of various uncertainties are integrated in a global design

resistance expressed by a global safety coefficient (1.27):

$$R_d = \frac{R(f_m,...)}{\gamma_R \gamma_{Rd}} = \frac{R(f_m,...)}{1.2 \cdot 1.06} = \frac{R(f_m,...)}{1.27} \qquad (17)$$

The ECOV method requires that two analyses are carried out, one with mean and one with characteristic mechanical properties of materials. It is based on the assumption of a lognormal distribution of the resistance; the coefficient of variation of resistance follows from the two calculated resistances:

$$R_m = R(f_m,...), R_k = R(f_k,...) \qquad (18)$$

$$R_d = \frac{R_m}{\gamma_R \gamma_{Rd}} \qquad (19)$$

$$\gamma_R = \exp(\alpha_R \beta V_R)$$
$$= \exp\left(0.8 \cdot 3.8 \cdot \left[\frac{1}{1.65} \ln(R_m/R_k)\right]\right) \qquad (20)$$

4 FINITE ELEMENT MODEL

Full 3D modeling is used. To model the concrete elements and steel plates 20-node brick elements with a ful Gaussian integration scheme (3x3x3) have been used; the average element's dimension is 110x100x100mm. For the reinforcement embedded truss elements with three Gaussian integration points along the axis of the element have been used; perfect bond has been assumed. For the dywidag bars truss elements have been used. Between the steel plates and the slab 16-node interface elements have been inserted.

Boundary conditions have been applied to the nodes of the steel plates and dywidag bars. Rigid movement of the slab in the x and y direction are prevented. The analyses comprise two phases. In the first phase the prestressing force in the dywidag bars (F_{pe}) and the dead load have been applied while in the second phase a displacement along z has been applied at the central node of the loading steel plate. The analyses have been carried out using a regular Newton-Raphson iteration scheme with a convergence criterion based on force and energy.

In Figure 8 a schematization of the mesh and boundary conditions are plotted for S1T1 slab, as example.
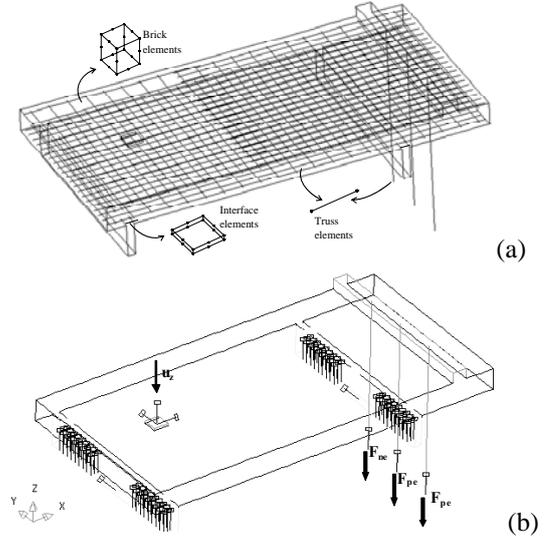
Figure 8: S1T1: (a) mesh, (b) boundary conditions.
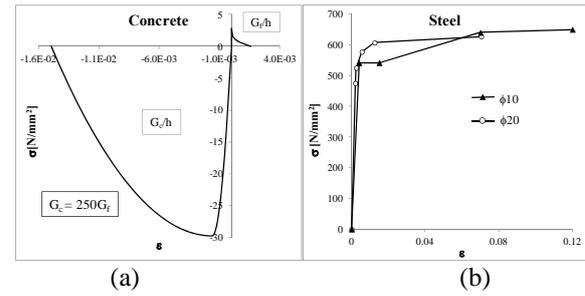
Figure 9: Constitutive model of (a) concrete and (b) steel.

For concrete a parabolic law in compression and an exponential law in tension have been used. For the reinforcement an elastic-plastic with hardening relation has been adopted, Figure 9. The constitutive laws of concrete are based on the definition of a compressive fracture energy and a tensile fracture energy, determined respectively according to [9] and [5]. Dywidag bars and steel plates have been modeled with a linear elastic behavior. Interfaces elements have been modeled with a nonlinear no-tension behavior, according to the experimental test, Figure 6.

Basic rotating and fixed crack models, implemented in several commercial software ([10], [11]), Various enhanced models ([12], [13], [14]) were not considered in this study.

In section 5 the effects of some parameters of the crack model used [7], like the Poisson effect, the shear retention factor function, the reduction of the compressive strenght due to lateral cracking etc. are investigated and further discussed.

5   MAIN RESULTS

NLFE analyses can provide refined models that are able to take into account hidden capacities of the structure, provided the validity and the reliability of the model used. If some parameters are not properly calibrated in the model a big scatter in the results can be found and the real load carrying capacity of the structure can be substantially overestimated or underestimated. Also for this reason the availability of guidance on how to perform NLFE analyses is helpul for users.

In Table 4 the main parameters investigated and combined in the analyses (Analysis A-F) are reported.

The variables listed in the table are described below:

- ν denotes the Poisson's ratio. The effect of a variable Poisson's ratio, that linearly decreases from its initial value (0.15) in the elastic phase down to zero in the cracked phase rather than a constant Poisson's ratio (equal to 0.15) has been investigated.
- $f_{c,red}/f_c$ denotes the limit to the reduction of the compressive strenght due to lateral cracking. In DIANA [7] the reduction trend of the compressive strenght due to lateral cracking follows the Model B of Vecchio & Collins [12], thus the compressive strengh is reduced due lateral cracking while the peak strain remains the same, leading to a reduction in the Young's modulus already in the elastic phase, Figure 10. More refined models would properly take into account the

decrease of both strenght and peak strain (e.g. [14]).

- G_f denotes the tensile fracture energy. In the analyses the value of G_f is calculated according to the new fib Model Code 2010 ($G_f=73f_c^{0.18}$), [5].
- G_c denotes the compressive fracture energy. The value of 250 G_f, suggested by [9], and a lower value (120 G_f) have been adopted in the analyses.
- β denotes the shear retention factor value. Analyses A, B, C and D have been carried out using a rotating crack model while Analyses E and F are using a fixed crack model, that requires the definition of a shear retention factor. In DIANA [7] a variable shear retention factor that linearly decreases from 1, in the elastic phase, down to 0.0 as the maximum crack width is equals to half of the aggregate size is implemented.
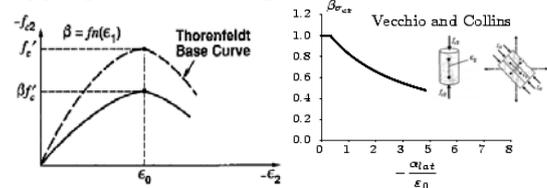
Figure 10: Reduction of the compressive strength due to lateral cracking according to the "Model B" of Vecchio et al. [12].

In Figure 11 the load-deflection curves obtained from the parametric study are reported. The parametric study for all slabs has been carried out inputting mean mechanical properties of materials, available from experimental tests.

From Figure 11 it can be noted the big influence of some parameters of the crack model on the results, especially in terms of obtained ultimate load values.

Table 4: Parametric study.

	ν	$f_{c,red}/f_c$	G_f	G_c	crack model	β
Analysis A	0.15	1	MC2010	$250G_{fMC2010}$	rotating	/
Analysis B	variable	1	MC2010	$250G_{fMC2010}$	rotating	/
Analysis C	variable	0.6	MC2010	$250G_{fMC2010}$	rotating	/
Analysis D	variable	0.6	MC2010	$120G_{fMC2010}$	rotating	/
Analysis E	variable	0.6	MC2010	$250G_{fMC2010}$	fixed	variable
Analysis F	variable	0.6	MC2010	$120G_{fMC2010}$	fixed	variable

When the fixed crack model was used a peak load value couldn't be detected. This is most likely due to stress locking in combination with the simplified model of the shear retention factor implemented in the software. It is of great importance, especially for shear critical specimens, that the shear retention factor trend is evaluated by the implementation with adequate laws that properly take into account the aggregate interlock phenomenon ([13], [15], [16], [17], [18]).

Within the rotating crack model the compressive fracture energy value, the Poisson's ratio trend and the reduction of the compressive strength due to lateral cracking gave a significant scatter in the results. Comparing analysis B and C it the influence of the reduction of the compressive strength due to lateral cracking becomes visible. The effect on the compression behavior of concrete is not justified by the type of failure of the slabs, but rather by the type of 3D modeling implemented in the software [7]. The modeling of the compressive behavior provides that the reduction of the compressive strength due to lateral cracking is equally applied in the three directions. This aspect should be further investigated in future research. Another important aspect is related to the maximum displacement obtained from the numerical simulations. The nonlinear finite element analyses seem to overestimate in all cases the ductility of the slabs. In this regard it is important to point out that the deformation of a slab, which is a very stiff structure, is sensitively influenced by the deformation of the supports. The deformation of the supports is tightly related to the modeling of the interface elements placed between the supports and the concrete slab. The behavior of the interface elements has been modeled according to experimental measurements (Figure 6) made on felt and felt/plywood, but it is also possible that the behavior of these layers substantially varied during the loading of the slabs.
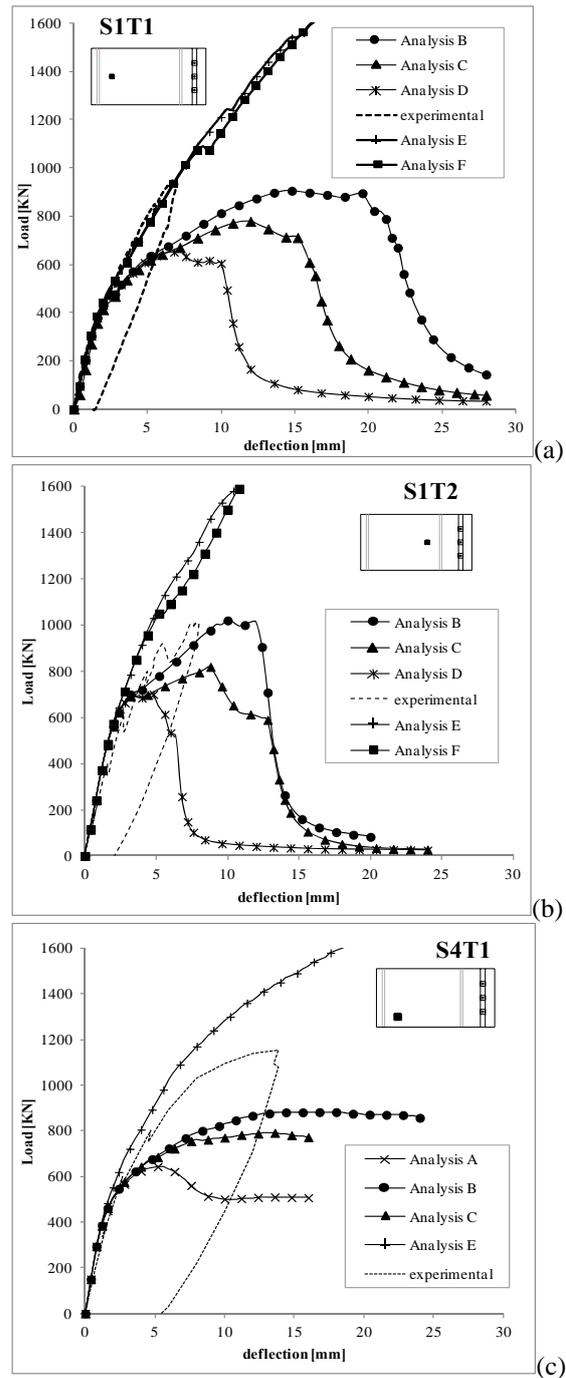
Figure 11: Load deflection curves obtained from the parametric study for (a) S1T1 slab, (b) S1T2 slab, (c) S4T1 slab.

From Figure 11 it can be noted that the load-deflection curve that best fits with the experimental curve, for all slabs, is Analysis B, which has been chosen as reference analysis for the safety format analyses. The parameters used in Analysis B are reasonable and rather

realistic with regards to the simplified crack model used.

In Figure 12 the tensile cracking strain values obtained from Analysis B for all slabs in correspondence of the peak load are plotted.

Comparing Figure 12 with Figure 3, Figure 4 and Figure 5 it can be noted that, also from NLFE analyses the failure mode observed can be related to a one-way shear failure rather than a punching shear failure.

(a)

(b)

(c)
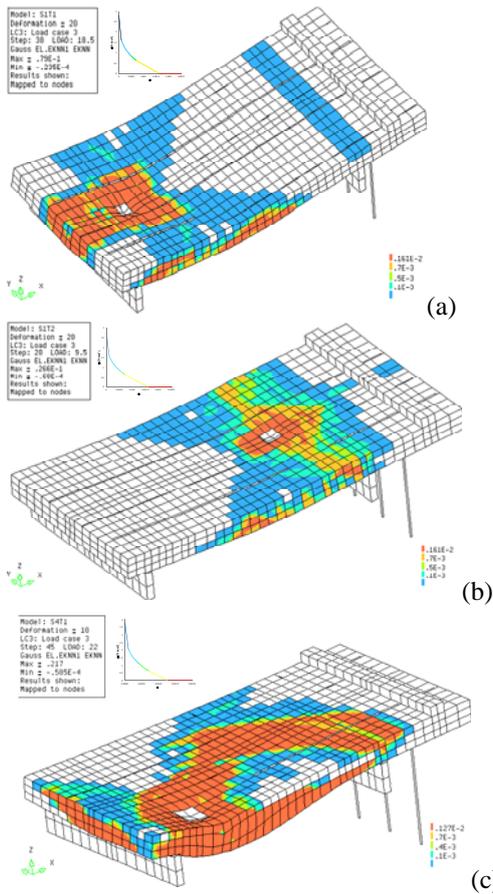
Figure 12: Tensile cracking strain development at peak load for (a) S1T1 slab, (b) S1T2 slab, (c) S4T1 slab.

In Figure 13 the design load values (P_u) derived from the shear resistance values calculated with analytical procedures (Level I-II) and numerical procedures (Level IV) are summarized. The ultimate design load values (P_u) are expressed as a percentage of the experimental ultimate load ($P_{u, exp}$) and plotted as histograms. In Figure 13 the ratio $P_u/P_{u,exp}$ of the reference analysis (Analysis B), carried out without applying the safety coefficient imposed by the safety format methods, is also plotted. The grey bars plotted in Figure 13

(Level I, Level II, Level IV PF, Level IV GRF, Level IV ECOV) refer therefore to the ratio between the design load values and the experimental load value, while the white bar (Analysis B) refers to the ratio between the peak load value, obtained from Analysis B, and the experimental value.

(a)

(b)

(c)
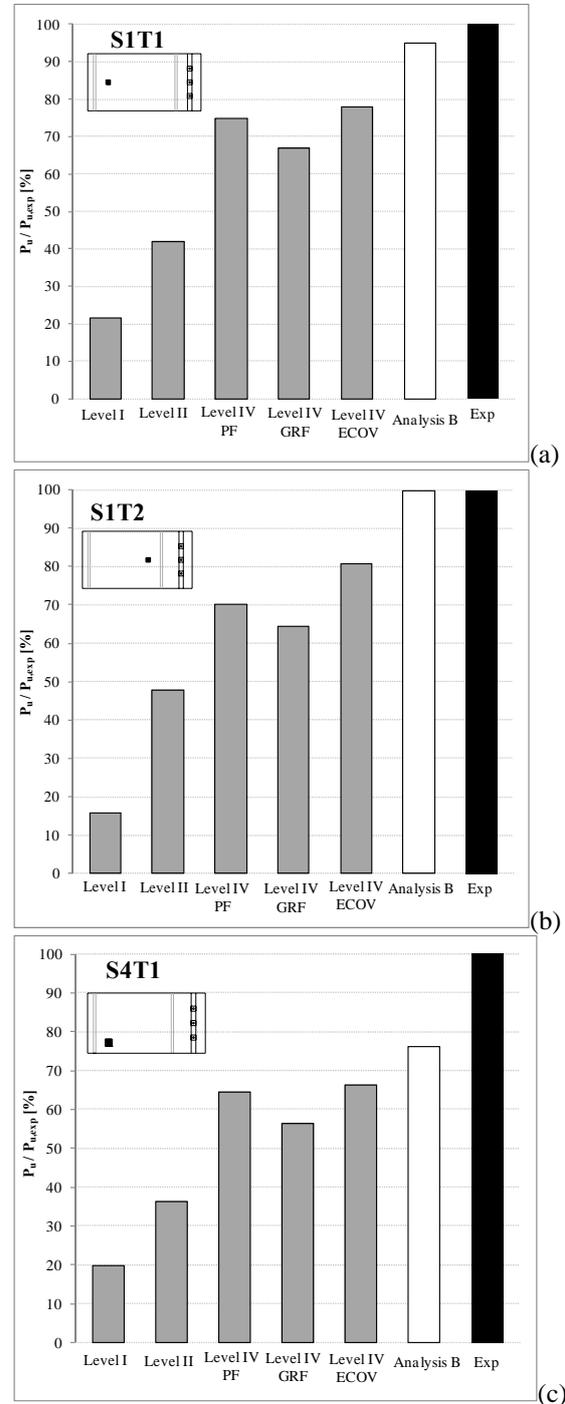
Figure 13: Design load values obtained analytically (Level I-II) and numerically (Level IV), expressed as a percentage of the experimental ultimate load $P_{u,exp}$ for (a) S1T1 slab, (b) S1T2 slab, (c) S4T1 slab.

From Figure 13 it can be noted that, as expected, the design load values are lower than the peak load value obtained from Analysis B, which does not apply any safety coefficient.

The trend of the results obtained with safety format methods well fits the new Model Code 2010 philosophy: by increasing the level of approximation the design load value increases. Level II provides a higher design load value than level I and level IV provides higher design load values than level I and II. A significant increase of the design load, ranging from 69% to 87%, can be detected from level II to level IV. This leads to confirm that, provided the validity of the numerical model used in the analyses, NLFE analyses can take more advantage of the hidden capacities of the structure. For this reason the availability of guidelines for NLFE analyses are helpful for the determination of the structural resistance. Furthermore the results obtained with level IV can be of use for intervention plans (e.g. maintenance, repair, demolition etc.) on existing structures.

6 CONCLUSIONS

In the paper the shear resistance of reinforced concrete slabs without shear reinforcement has been evaluated according to the calculation methods proposed by the new Model Code 2010. Three reinforced concrete slabs, tested at the Stevin laboratory [6], have been analyzed with analytical and numerical procedures and the results obtained have been compared with the experimental results.

The main results of the research are listed below.

- According to the new Model Code 2010 the design shear resistance of reinforced concrete slabs can be evaluated through different levels of approximation related to analytical and numerical procedures. By increasing the level of approximation the complexity and the accuracy of the shear resistance increases.
- The results obtained well fit with the philosophy of the new Model Code 2010. Level of approximation IV, determined from NLFE analyses results, properly reduced in order to obtain the same safety level of analytical procedures, provides substantially higher design shear resistance values than the shear resistance value obtained from analytical calculations.
- The design shear resistance values determined with Level IV are derived following the Dutch guidelines for nonlinear finite element analyses [2] and are based on relatively simple crack models.
- The results obtained from NLFE analyses can strongly depend on the modeling choices made by the analyst during the analyses, especially with regards to some aspects related to the crack model used. The availability of guidance on how to properly perform NLFE analyses is therefore important.
- All level IV results obtained give a "safe-side" estimation of the design shear resistance.
- In the authors' experience, the structural assessment of RC slabs is however less accurate than the structural assessment of RC beams [3], [4]. This is also due to the fact that the implementation of crack models in 3D is more complex than in 2D. Further experimental, theoretical and numerical research should be developed for the 3D modeling of the non-linear behavior of reinforced concrete.
- The analyst has to be able to critically validate input and output. To this aim the importance of a good knowledge of both physical phenomena and software modeling is underlined.
- The structural assessment carried out with the levels of approximation can moreover be of use for intervention plans on existing structures (e.g. maintenance, repair, demolition etc.).

REFERENCES

[1] EN 1992-1 (2004) Eurocode2: Design of concrete structures. Part 1: General rules and rules for buildings.

[2] Hendriks, M.A.N., den Uijl, J.A., de Boer, A., Feenstra, P.H., Belletti, B., Damoni, C., 2012. Guidelines for non-linear finite element analyses of concrete structures. Rijkswaterstaat Technisch Document (RTD), Rijkswaterstaat Centre for Infrastructure, RTD:1016:2012.

[3] Belletti, B, Damoni, C, Hendriks, M.A.N. 2011. Development of guidelines for nonlinear finite element analyses of existing reinforced and pre-stressed beams. *European Journal of Environmental and Civil Engineering*, **15** (9):1361-1384.

[4] Rots, J., Belletti, B., Damoni, C., Hendriks, M.A.N. Development of Dutch guidelines for nonlinear finite element analyses of shear critical bridge and viaduct beams. fib Bulletin 57: Shear and punching shear in RC and FRC elements, pp. 139-154.

[5] ceb-fip bulletin d'information 65&66 - Model Code MC2010 - Final Draft, International Federation for Structural Concrete (fib), Lausanne, Switzerland. 2012.

[6] Lantsoght, E., 2012. Shear tests of Reinforced Concrete Slabs Experimental data of Undamaged Slabs 06-01-2012. Technical Report, Stevin laboratory, Delft University of Technology.

[7] Manie, J. 2009. DIANA user's manual. TNO DIANA BV.

[8] Regan, P.E., 1982. Shear resistance of Concrete Slabs at Concentrated Loads close to Supports. Engineering Structures Research Group, Polytechnic of Central London, London, UK, pp. 24.

[9] Nakamura, H., Higai, T., 2001. Compressive Fracture Energy and Fracture Zone Length of Concrete. Benson P. Shing (eds), pp. 471-487.

[10] Feenstra, P.H., Rots, J.G., Arnesen, A., Teigen, J.G., Høiseth, K.V., 1998 . A 3D constitutive model for concrete based on a co-rotational concept. *Computational Modelling of Structures*, de Borst, Bicanic, Mang & Meschke (eds), Balkema.

[11] Cervenka, V., 1985. Constitutive model for cracked reinforced concrete. *ACI Struct. Journal*, **71**:396-408.

[12] Vecchio, F.J., Collins, M.P., 1986. The modified compression-field theory for reinforced concrete elements subjected to shear. *ACI Struct. Journal*, **83**(2):219-231.

[13] Belletti, B., Cerioni, R., Iori, I. 2001. A Physical Approach for Reinforced Concrete (PARC) membrane elements. *J. Struct. Eng.*, **127**(12):1412-1426.

[14] Belarbi, A., Hsu, T.T.C., 1991. Constitutive laws of reinforced concrete in biaxial tension-compression. *Research Report UHCEE 91-2*, University of Houston.

[15] Walraven, J.C., 1981. Fundamental analysis of aggregate interlock. *J. Struct. Eng.*, **107**(11):2245-2270.

[16] Gambarova, P.G., 1983. Sulla trasmissione del taglio in elementi bi-dimensionali piani in c.a. fessurati. *Proc. Giornate AICAP*, (in Italian).

[17] Walraven, J.c., Belletti, B., Esposito, R., 2012. Shear capacity of normal, lightweight & high-strength concrete beams according to MC2010. Part I., *J. Struct. Eng.*, in press.

[18] Belletti, B., Esposito, R., Walraven, J.C.,2012. Shear capacity of normal, lightweight & high-strength concrete beams according to MC2010. Part II. , *J. Struct. Eng.*, in press.